Evolution of a magnetic order in the quasi-kagome lattice system $CeRh_{1-x}Pd_xSn$ ($x \leq 0.75$)

C L Yang[1], K Umeo[2] and T Takabatake[1,3]

[1] Graduate School of Advanced Sciences of Matter, Hiroshima University, Higashi-Hiroshima 739-8530, Japan
[2] Natural Science Center for Basic Research and Development, Hiroshima University, Higashi-Hiroshima 739-8526, Japan
[3] Institute for Advanced Materials Research, Hiroshima University, Higashi-Hiroshima 739-8530, Japan

takaba@hiroshima-u.ac.jp

Abstract. The equiatomic compound CeRhSn with a quasi-kagome lattice of Ce atoms displays a non-Fermi liquid behavior at low temperatures. We have studied how the ground state changes with the substitution of Pd for Rh in $CeRh_{1-x}Pd_xSn$ ($0 \leq x \leq 0.75$) by measuring the specific heat C, magnetic susceptibility χ, and magnetization M. With increasing x, the lattice parameters a and c increase by 1.6%, the paramagnetic Curie temperature in $\chi(T)$ changes from −112 K to 16 K, and $M(B = 5\ \mathrm{T})$ at $T = 1.8$ K increases from $0.05\mu_B$/Ce to $1.4\mu_B$/Ce. A long-range magnetic order manifests in sharp peaks in C at 0.7, 1.0 and 1.5 K for $x = 0.4$, 0.5 and 0.65, respectively. An antiferromagnetic order for $x = 0.75$ is indicated by the observations of peaks in both $\chi(T)$ and $C(T)$ at around 3.0 K and metamagnetic behavior in $M(B)$ at $B = 2$ T. Our results point out that the doping of 4*d* electrons in the non-Fermi liquid system CeRhSn destroys the coherence of the quasi-kagome lattice and weakens the hybridization between the 4*f* state and conduction bands, leading to the evolution of antiferromagnetic order.

1. Introduction

Quantum phase transitions in the 4*f* electron systems have fascinated physicists for decades because they involve competition and/or coexistence of magnetic order, non-Fermi liquid (NFL) state, and unconventional superconductivity [1,2]. Conventional quantum criticality at zero temperature can be reached by tuning the coupling between the 4*f* electron and conduction electrons governing the competition between RKKY-interaction and Kondo effect, well known as the Doniach phase diagram [3]. The ordinary ways to tune the balance of the two interactions are through chemical composition, pressure, and magnetic field, leading from a magnetically ordered state to a paramagnetic one [4]. Recently, a kagome lattice of 4*f* elements with antiferromagnetic nearest neighbor interaction due to the triangular-like geometry is reported to induce an unconventional quantum critical point [5-12]. In this system the competition occurs between a spin liquid state and a Kondo singlet state, which is caused by the interplay among the RKKY-interaction, Kondo effect, and magnetic frustration [13,14]. Hence, a long-range order can be induced by either destruction of symmetry of frustrated structure or breakdown of Kondo screening behavior.

CePdAl has a quasi-kagome lattice of Ce ions in the hexagonal ZrNiAl-type structure [5,15,16]. Within a single quasi-kagome layer, only two thirds of Ce moments participating in the

antiferromagnetic (AFM) long-range order occurring at T_N = 2.7 K, while the others remain paramagnetic [6]. By doping with Ni for Pd, the AFM order in $CePd_{1-x}Ni_xAl$ is completely suppressed at x = 0.144. The frustrated Ce moments give rise to a two dimensional quantum critical point (QCP) [9]. The ratio $|\theta_p|/T_N$, where θ_p is the paramagnetic Curie temperature in the magnetic susceptibility χ, increases with x as the Kondo effect surpasses the RKKY-interaction. Another example with QCP is the isostructural alloy system $CeRh_{1-x}Pd_xIn$, in which a mixed valence state changes to an AFM heavy fermion state [12]. Then, an AFM order appears for x = 0.8 at T_N = 0.65 K which rises to 1.7 K for x = 1. Thereby, the increase in the 4*d*-electron number deepens the 4*f* level from the Fermi level suppressing the hybridization between 4*f* states of Ce and 4*d* states.

In the isostructural compound CeRhSn, layers composed of Ce and Rh1 atoms alternate along the *c* axis with layers composed of Rh2 and Sn atoms as shown in insert of Figure 1 [11]. Nearest neighbors for the Ce atom are four Rh2 atoms and the second nearest neighbor is one Rh1 atom. This structural aspect suggested that the Ce 4*f* state is strongly hybridized with the 4*d* band derived mainly from the Rh2 atoms, leading to the valence-fluctuating state with a high Kondo temperature T_K ~ 200 K. Below 7 K, however, NFL behavior appear: $\chi(T)$ shows a power-law behavior, $\rho(T)$ decreases with T^n ($n \leq 1.5$), and the specific heat divided by temperature C/T shows an upturn and saturation to a large value of 200 mJ/K^{2}mol. These evident NFL behaviors are thought to be manifestation of the frustration of Ce moments which hinders the long-range order and leads to a QCP. Furthermore, a zero-field QCP in CeRhSn has been indicated by the measurements of *C*, uniaxial thermal expansion, and magnetic Grüneisen parameter [17]. The anisotropy of thermal expansion displaying the critical behavior only along the *a* axis is in support of the fact that the quantum criticality is driven by geometrical frustration in the quasi-kagome lattice.

Recently, it has been reported that the alloy $CeRh_{1-x}Pd_xSn$ maintains the ZrNiAl-type structure up to x = 0.8 [18]. In the whole range, no magnetic order was found down to 2.5 K in the measurements of $\chi(T)$. We expected that the destruction of the local symmetry of the frustrated structure should induce a magnetic order. Therefore, we have studied the magnetic properties down to 0.4 K in this work.

2. Experiment

Polycrystalline samples with initial compositions of $CeRh_{1-X}Pd_XSn$ (X = 0, 0.2, 0.3, 0.4, 0.5, 0.7, 0.8) were prepared by arc-melting appropriate amounts of constituent elements Ce (99.9%), Rh (99.9%), Pd (99.99%) and Sn (99.999%) under a pure argon atmosphere. In order to improve the homogeneity, these samples were turned over after melting and remelted for several times, and were subsequently annealed at 900℃ for 6 days in evacuated quartz ampoules. Total weight loss after preparation was not above 1%. The samples were characterized by powder X-ray diffraction and wavelength dispersive electron-probe microanalysis (EPMA). Lattice parameters of the ZrNiAl-type structure were calculated by least-square refinements of the XRD patterns. The metallographic examination showed that the polycrystalline samples are composed of grains preferentially oriented along the *c* axis, which is perpendicular to the bottom of the ingot. For the measurements of $\chi(T)$ and magnetization $M(B)$, the magnetic field was applied along the preferentially oriented *c* axis of the samples which were cut perpendicularly to the bottom. The measurements were performed in the temperature range from 1.8 to 300 K with a Quantum Design MPMS. The specific heat was measured on 10 mg samples from 0.4 to 20 K by the relaxation method in a Quantum Design PPMS.

3. Results and discussion

3.1. Chemical and structural properties

The results of EPMA are consistent with the nominal composition for $X \leq 0.5$. However, with increasing X, the quantity of impure phase $Ce(Rh_{1-X}Pd_X)_2Sn_2$ increased. The real compositions of Pd, x, in $CeRh_{1-x}Pd_xSn$ phase were found to be 0.65 and 0.75 for X = 0.7 and 0.8, respectively. The hexagonal

lattice parameters *a* and *c* of CeRhSn agree with the reported values [18]. As shown in Figure 1, the *a* parameter linearly increases as *x* increases from 0 to 0.75, while the *x* dependence of the *c* parameter deviates upward from the Vegard's law, in consistent with the previous report [18]. This deviation hints a change in the 4*f* state from the valence fluctuating state to the localized state, which is consistent with the results of magnetic susceptibility and magnetization as will be shown in the next subsections. The expansion along the *c* axis enlarges the distance between Ce and Rh2 out of basal plane, which may decrease the overlap of wave functions between the 4*f* electron and the 4*d* electron. Nevertheless, local extension in the basal plane may break the symmetry of the quasi-kagome lattice of Ce atoms.

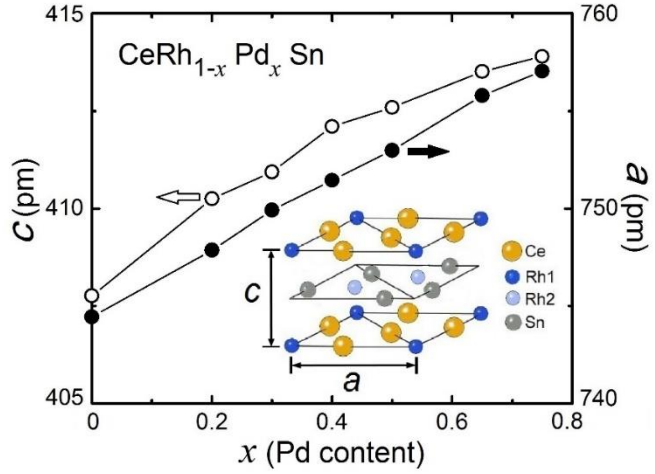

Figure 1. Hexagonal lattice parameters of $CeRh_{1-x}Pd_xSn$ as a function of *x*. The insert shows the unit cell of CeRhSn [11].

3.2. Magnetic properties

Figure 2 shows the inverse susceptibility as a function of temperature for $CeRh_{1-x}Pd_xSn$ ($x \leq 0.75$) measured in a magnetic field of 1 T. The solid lines at $T > 100$ K represent the Curie-Weiss fit with $\chi = C/(T - \theta_p) + \chi_0$, where the last term represents the temperature independent contribution. For $x = 0$, the large negative value of paramagnetic Curie temperature $\theta_p = -112$ K and effective magnetic moment

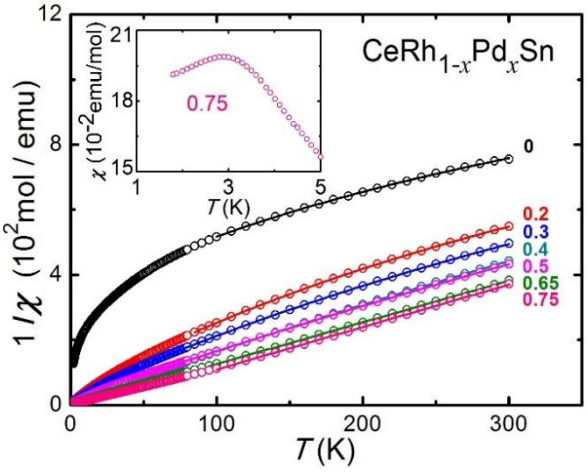

Figure 2. Temperature dependence of the inverse susceptibility of $CeRh_{1-x}Pd_xSn$. Solid lines are Curie-Weiss fits to the data at temperatures above 100 K.

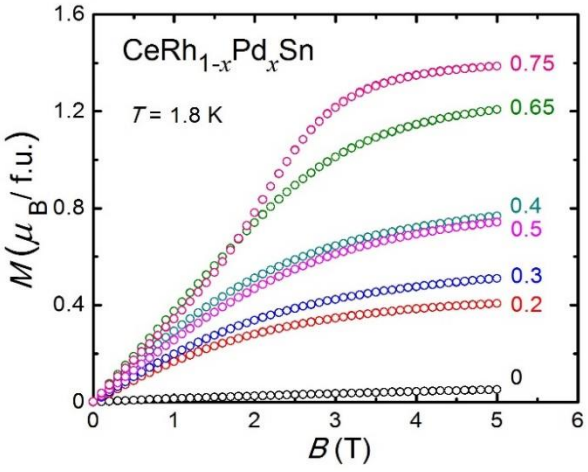

Figure 3. Magnetization of $CeRh_{1-x}Pd_xSn$ as a function of the magnetic field at 1.8 K.

$\mu_{\rm eff} = 1.47\mu_B$ are characteristics for a valence fluctuation system. With the increase in x to 0.2, the value of $|\theta_{\rm p}|$ decreases to 13 K. This decreasing trend in $|\theta_{\rm p}|$ suggests that the hybridization is weakened as $|\theta_{\rm p}|/2$ is a measure of $T_{\rm K}$ [19]. The sign of $\theta_{\rm p}$ becomes positive for $x \geq 0.65$, which can be attributed either to the crystal field effect on nearly trivalent Ce ions or possible ferromagnetic interaction due to the increase in the Fermi wave vector. For $x \geq 0.65$, $\mu_{\rm eff}$ increases to 2.50$\mu_{\rm B}$/Ce, which value is close to 2.54$\mu_{\rm B}$ expected for a free Ce^{+3} ion. As shown in the inset of Figure 2, the data of $\chi(T)$ for x = 0.75 exhibits an obvious maximum at around 3 K, suggesting an antiferromagnetic order.

The magnetization curves $M(B)$ measured in fields up to 5 T at T = 1.8 K are shown in Figure 3. For x = 0, $M(B)$ increases almost linearly, yielding a value of 0.05$\mu_{\rm B}$/Ce at 5 T. This value is 67% of that reported on the single crystal for B // c, confirming the preferred orientation of grains along the c axis in the polycrystal. For $x \geq 0.2$, $M(B)$ gradually increases and shows a tendency towards saturation. Especially, $M(B)$ for x = 0.75 shows a spin-flop behaviour at B = 2 T and reaches a saturated value of 1.4 $\mu_{\rm B}$/Ce at 5 T. Under the hexagonal symmetry, the J = 5/2 multiplet of the 4f state splits into three doublets. The magnitude of 1.4 $\mu_{\rm B}$/Ce is 67% of the value 2.14 $\mu_{\rm B}$/Ce for a ground state doublet with $J_{\rm Z}$ = ±5/2. This fact indicates that the hybridization between 4f states of Ce and 4d states of Rh2 is weakened because the 4d electron doping lowers the energy level of 4f state from the Fermi level.

3.3. Specific heat

The data of specific heat C between 0.4 K and 20 K are plotted as C/T vs log$T$ in Figure 4. For x = 0, C/T linearly increases on cooling below 7 K and saturates to a value γ = 290 mJ/K^{2}mol, in agreement with the behaviour reported for a single crystal [11]. For x = 0.2 and 0.3, pronounced upturns suggest the approach to a QCP. For x $\geqslant$ 0.4, the C/T data exhibit peaks, whose temperatures are taken as $T_{\rm N}$. The $T_{\rm N}$ increases from 0.7 K for x = 0.4 to 1.5 K for x = 0.65, indicating the enhancement of AF

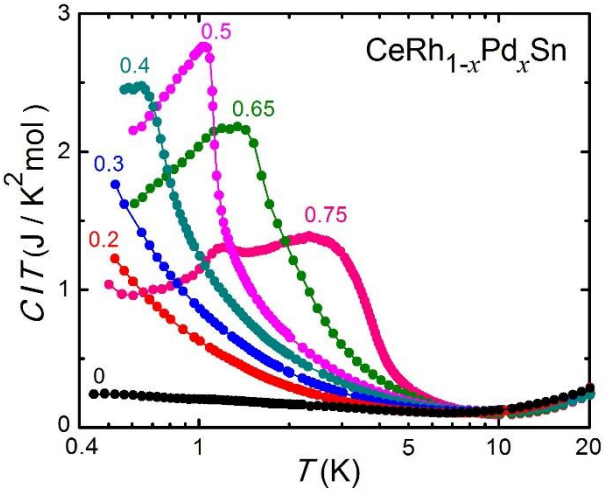

Figure 4. Specific heat of $CeRh_{1-x}Pd_xSn$ plotted as C/T vs log$T$.

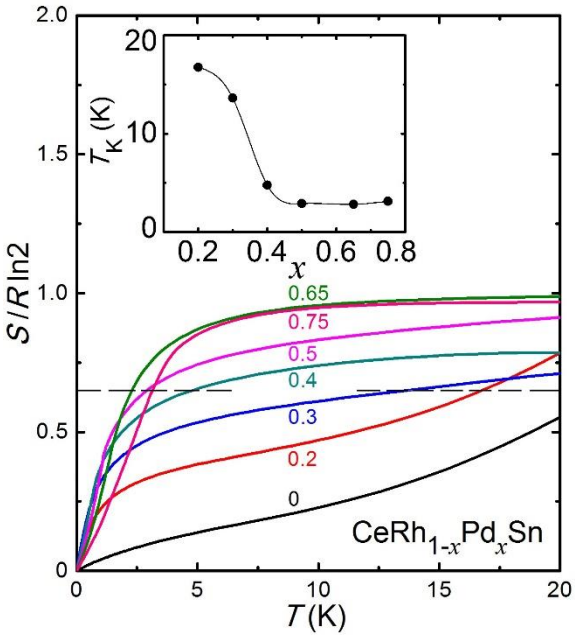

Figure 5. Magnetic entropy of $CeRh_{1-x}Pd_xSn$ as a function of temperature. The dotted line represents the value of 0.65Rln2. The insert shows the x dependence of Kondo temperature $T_{\rm K}$.

interaction and/or growth of magnetic moments. For $x = 0.75$, two maxima are found at 1.2 K and 3 K. The latter one is identified as T_N because it agrees with the maximum temperature in $\chi(T)$. It is noted that the peaks in the C/T data broaden with increasing x from 0.4 to 0.75. The magnetic structure in this system should be further studied by the neutron diffraction experiment.

In order to obtain the magnetic entropy $S(T)$, specific data of $CeRh_{1-x}Pd_xSn$ for $0 \leq x \leq 0.3$ and $0.4 \leq x \leq 0.75$ were extrapolated, respectively, with the equations $C/T = \gamma + \beta T^2 + CT^2 \ln T$ [20] and $C/T = \gamma + \beta T^2 + \delta T^2 e^{-\Delta/k_B T}$ [21]. The data of isostructural LaRhSn were used as the phonon contribution. The temperature dependences of $S(T)$ are plotted in Figure 5. The $S(T)$ curves for $x = 0.65$ and 0.75 are saturated to $R\ln 2$ at 20 K, confirming the doublet ground state under the crystal field. The T_K was estimated by the relationship $S(T_K) = 0.65R\ln 2$, which was given for a Kondo impurity [22,23]. The values of T_K as a function of x are shown in insert. The T_K decreases rapidly from 16 K for $x = 0.2$ to 5 K for $x = 0.4$, indicating the strong suppression of Kondo effect.

4. Conclusions

We have reported a set of measurements on X-ray diffraction, magnetic susceptibility, magnetization, and specific heat for $CeRh_{1-x}Pd_xSn$ series in which the Ce atoms form a quasi-kagome lattice. With increasing x up to 0.75, which is the limit for the ZrNiAl-type structure, lattice parameters a and c increase by 1.6%. The 4*f* state of Ce ion changes from a valence fluctuating state to a stable trivalent state with a doublet ground state. Importantly, the specific data show apparent maximum in C/T for $x \geq 0.4$. The spin-flop behaviour in the magnetization curve and the peak in $\chi(T)$ for $x = 0.75$ supports the AFM ordered state. The AFM order may be induced by the combination of two mechanisms. On one hand, the increasing c axis parameter and additional 4*d* electrons weaken the hybridization between 4*f* orbitals of Ce and 4*d* orbitals of Rh2. As a result, the magnetic moment is increased and thus the RKKY interaction is enhanced. On the other hand, local extension in the basal plane near the Pd atoms may break the symmetry of the quasi-kagome lattice of Ce atoms, then the frustrated Ce moments have the chance to be coupled antiparallel. In any case, we have found that the NFL state of CeRhSn is easily transformed to an AFM ordered state. For the study of quantum phase transition, the system $CeRh_{1-x}Pd_xSn$ deserves to be further studied by neutron scattering and μSR experiments.

Acknowledgements

This work was partly supported by KAKENHI Grant Numbers Nos. 26400363 and 16H01076.

References

[1] Si Q, Pixley J H, Nica E, Yamamoto S J, Goswami P, Yu R and Kirchner S 2014 *J. Phys. Soc. Jpn.* **83** 0061005, and references therein
[2] Gegenwart P, Si Q and Steglich F 2008 *Nat. Phys.* **4** 186
[3] Doniach S 1977 *Physica B* **91** 231
[4] Löhneysen H v, Rosch A, Vojta M and Wölfle P 2007 *Rev. Mod. Phys.* **79** 1015
[5] Kitazawa H, Matsushita A, Matsumoto T and Suzuki T 1994 *Physica B* **199-200** 28
[6] Dönni A, Ehlers G, Maletta H, Fischer P, Kitazawa and Zolliker M 1996 *J. Phys.: Condens. Matter* **8** 11213
[7] Goto T, Hane S, Umeo K, Takabatake T and Isikawa Y 2002 *J. Phys. Chem. Solids* **63** 1159
[8] Oyamada A, Maegawa S, Nishiyama M, Kitazawa H and Isikawa Y 2008 *Phys. Rev. B* **77** 064432
[9] Fritsch V, Bagrets N, Goll G, Kittler W, Wolf M J, Grube K, Huang C L and Löhneysen H v 2014 *Phys. Rev. B* **89** 054416
[10] Fritsch V *et al*. 2015 *Eur. Phys. J. Special Topics* **224** 997
[11] Kim M S *et al*. 2003 *Phys. Rev. B* **68** 054416
[12] Brück E, Nakotte H, Bakker K, de Boer F R, de Châtel P F, Li J Y, Kuang J P and Yang F M 1993 *J. Alloys Comp.* **200** 79
[13] Vojta M 2008 *Phys. Rev. B* **78** 125109.

[14] Coleman P and Nevidomskyy A H 2010 *J. Low Temp. Phys.* **161** 182
[15] Woitschach S, Stockert O, Koza M M, Fritsch V, Löhneysen H v and Steglich F 2013 *Phys. Status Solidi B* **250** 468
[16] Fritsch V, Huang C L, Bagrets N, Grube K, Schumann S and Löhneysen H v 2013 *Phys. Status Solidi B* **250** 506
[17] Tokiwa Y, Stingl C, Kim M S, Takabatake T and Gegenwart P 2015 *Sci. Adv.* **1** e1500001
[18] Niehaus O, Abdala P M and Pöttgen R 2015 *Z. Naturforsch.* **70** 253
[19] Gignoux D and Gomez-Sal J C 1984 *Phys. Rev. B* **30** 3967
[20] Brodsky M B 1978 *Rep. Prog. Phys.* **41** 1547
[21] Cooper B R 1962 *Proc. Phys. Soc.* **80** 1225
[22] Desgranges H U and Schotte K D 1982 *Phys. Lett.* **91** 240
[23] Bredl C D, Steglich F and Schotte K D 1978 *Z. Phys. B* **29** 327